MECHANICAL MODULI OF AORTA AND IT'S ARTIFICIAL SUBSTITUTES

J. Polanský**, O. Boiron***, A. Lescaille**** and V. Nováček*

* University of West Bohemia/Department of Mechanics, Plzeň, Czech Republic
** University of West Bohemia/Department of Power System Engineering, Plzeň, Czech Republic
*** EGIM – IRPHE, IMT, Technopôle de Château-Gombert, Marseille, France
**** Institut Supérieur des Bio Sciences, Paris, France

polansky@kke.zcu.cz, olivier.boiron@egim-mrs.fr, aude.lescaille@voila.fr, vnovacek@kme.zcu.cz

Abstract: An experimental method was proposed in order to determine the material moduli of estan and silicon which represent the artificial materials of a vascular wall tissue. Various models of the blood vessels were prepared from these materials for the experimental study of a blood flow using PIV (Particle Image Velocimetry) and UVP (Ultrasound Velocity Profilometry) methods. Material moduli are necessary for the further investigation of the flow-structure interaction. Porcine aortic tissue was examined as well to compare the properties of the real and artificial materials. Viscoelastic and hyperelastic models were applied to fit the experimental data and to obtain the material moduli.

Introduction

Estan and silicon are materials appropriate for physical models of vascular vessel wall intended for experiments using PIV (Particle Image Velocimetry) and UVP (Ultrasound Velocity Profilometry) techniques. These experiments investigate the flow through various parts of the blood vessels and help to understand better various physiological and pathological phenomena (i.e. atherosclerothic disease, aneurisma, etc.). To compare the mechanical properties of physical models mentioned above and real tissue, simple traction experiment is proposed. Estan, silicon and porcine aorta samples undergo the mechanical testing. The experimental data are examined and fitted to viscoelastic and/or hyperelastic models. As a result of the fitting process, a set of material moduli is obtained. These

Figure 1: Estan model of vascular vessels.

material moduli characterize the mechanical properties of the material under consideration.

The models should be predictive in such a way that using the determined material moduli and prescribing new boundary conditions, i.e. the deformation of the sample, the models should give appropriate and credible resulting stress/force evolution in time. They should also indicate the suitable model of the vessels, that is type of silicon or estan, number of layers, technology of preparation, etc.

Previously, vascular wall was experimenally studied in [3]. Incremental stress-relaxation measurements were made on strips of relaxed smooth muscle excised from cerebral vessels. Generalized Maxwell models are applied to fit the experimental data and to obtain the viscoelastic moduli. Similar method was adopted in this work.

Materials and Methods

Estan and silicon flat specimens were cut from the physical models in three different directions (see Figure 2). The initial dimensions of the specimens are as follows: 100 mm length, 54 mm width, 0.42 mm thickness, giving the total cross-section area 22.68 mm^2. Each sam-

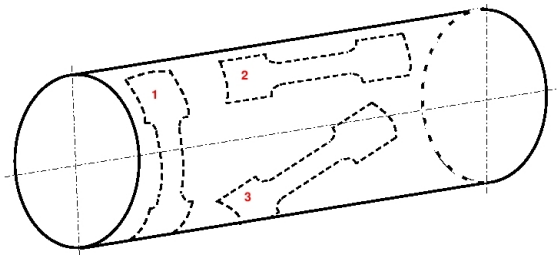

Figure 2: Estan and silicon specimens' shape.

ple was loaded in traction according to measuring protocol. In this stress-relaxation experiment, constant strain increment was prescribed and stress was recorded (see Figure 3). The experimental data were processed in MATLAB®. Recorder data were filtered to reduce the noise of the output signal.

Measuring apparatus was designed and constructed at the laboratory of l'Equipe de biomécanique cardiovasculaire of IRPHE, Marseille. The scheme of the measuring apparatus is presented on the Figure 4. The apparatus allows to test flat samples and tube specimens with the internal pressure applied. The actual width of a flat sample

ISSN: 1727-1983

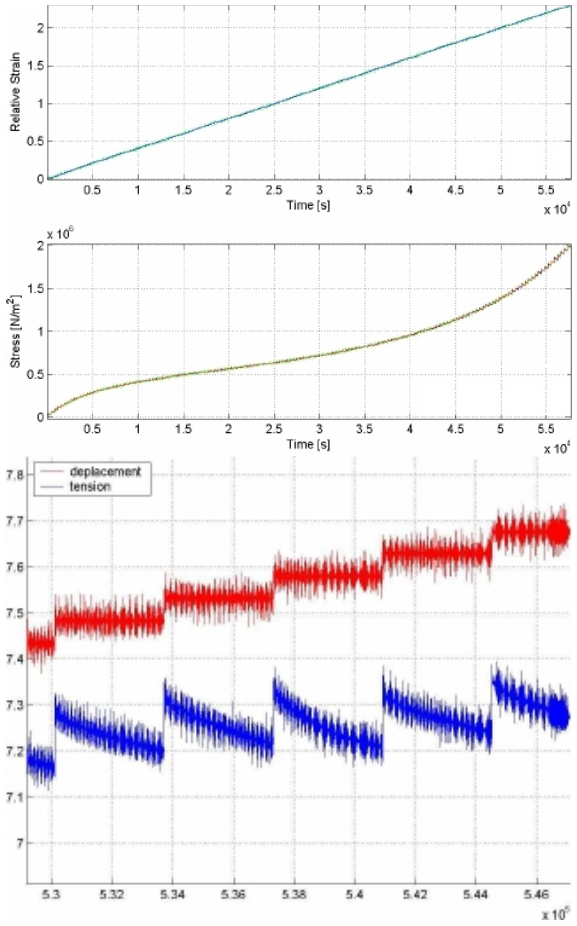

Figure 3: Strain and stress evolution in time and detail view of the displacement and tension data.

is registred by camera.

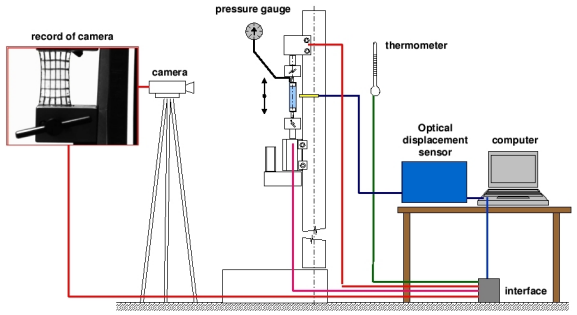

Figure 4: Scheme of measuring apparatus.

As a preliminary study, porcine abdominal aorta samples were tested as well to obtain the stress-strain relation. Strips of the tissue were cut off the aorta and glued between two metal plates, than inserted between the jaws of the traction machine. The tissue was not kept in any solution during testing to prevent drying of the sample since the apparatus does not allow this option yet. Continuous elongation was prescribed as a boundary condition up to the rupture of the specimen to obtain the relation between Green strain and Kirchhoff stress. This relation was not fitted with any constitutive law and material parameters

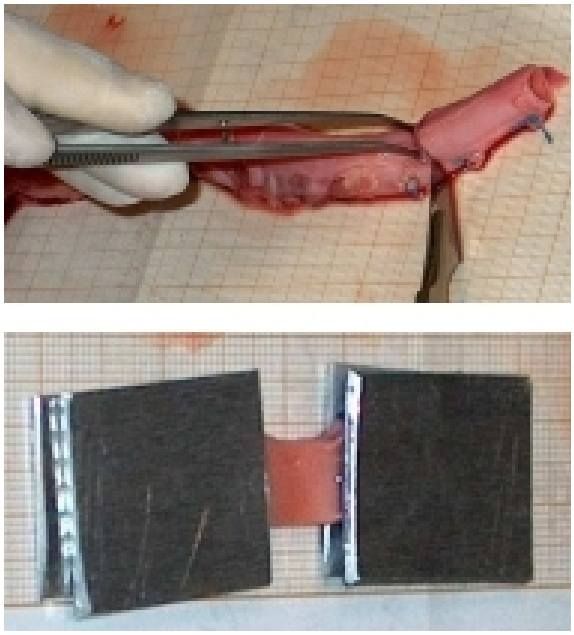

Figure 5: Aorta sample preparation.

were not identified since the experiments on aorta are considered as a preliminary study only. This should be done in the nearest future to compare the properties of the artificial and real materials.

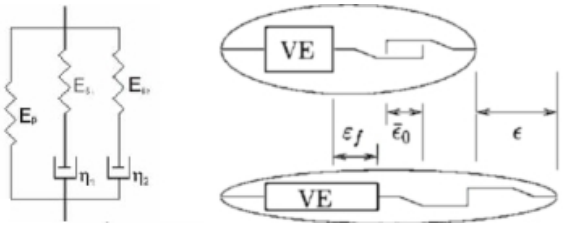

Figure 6: Left: 5-parameters Maxwell model. Right: Slack length element.

First model, selected for material data indentification of the estan and silicon material, was generalized Maxwell model with k branches, i.e. simple viscoelastic 1D model composed of springs and dashpots. Relaxation of this model is described by stress evolution in time as follows

$$\sigma(t) = E_P\varepsilon + \sum_{k=1}^{n} E_S^k \varepsilon \exp\left(-t/\tau_k\right), \qquad (1)$$

where E_P is an elastic modulus of a single paralel spring, E_S^k is the elastic modulus of the k-th spring-dashpot branch, $\tau_k = \eta_k/E_S^k$ is the relaxation time of the k-th branch, η^k is the viscosity of the k-th dashpot, ε is strain increment and t is time. Up to five element model was used.

To treat the assumed viscoelasticity, generalized nonlinear 3-parameter model with a slack length element was also applied. This model allows to introduce large deformations via strain energy term. Slack length element expresses the fact that the material can transmit only tension

ISSN: 1727-1983

but no compression. In fact, it is the uniaxial Kelvin (3 parametric) model with the discrete relaxation spectrum (i.e. structural damping sensitive to frequency of loading). For more details, see e.g. [1, 4]. The viscoelastic stress τ is a function of the (nonlinear) elastic response σ and the internal stress-like variable q, such that the following equation holds $\tau = \sigma - q$. Non-linear response is expressed in terms of the strain potential function w,

$$\sigma = \frac{\partial}{\partial \varepsilon} w(\varepsilon), \tag{2}$$

The internal variable q satisfies

$$\dot{q} + \frac{1}{t_\varepsilon} q = \frac{\gamma}{t_\varepsilon}\sigma, \quad \lim_{t\to-\infty} q(t) = 0, \tag{3}$$

with non-dimensional relative moduli (between 0 and 1)

$$\gamma = \frac{E}{E+E_\infty}, \quad \gamma_\infty = \frac{E_\infty}{E+E_\infty}, \quad \gamma+\gamma_\infty = 1. \tag{4}$$

Relaxation times may be defined as

$$t_\varepsilon = \frac{\eta}{E}, \quad t_\sigma = \frac{t_\varepsilon}{1-\gamma} \tag{5}$$

where E is the elastic modulus connected in serie with the viscous element η, E_∞ is the elastic modulus connected in parallel to them. Eliminating q leads to governing differential equation

$$\tau + t_\varepsilon \frac{d\tau}{dt} = (1-\gamma)(\sigma + t_\sigma \frac{d\sigma}{dt}). \tag{6}$$

The explicit formula for σ may be derived as follows

$$\sigma(t) = \bar{\gamma}\left[\tau(t) - \gamma \int_{t_0}^{t} \exp[-\beta(t-s)]\frac{d}{ds}\tau(s)ds\right] \tag{7}$$

where $\bar{\gamma} = 1/(1-\gamma)$. Choosing the appropriate form of the energy potential $w(\varepsilon)$ leads to various models. Note that the quadratic form leads to the standard linear solid model. Introducing the slack length parameter allows the material to transmit tension only after its straightening while in compression it cannot transmit any load. This behaviour results in the fact that the bulk stiffness of the material increases as the stretch progresses. This is a behaviour of e.g. collagen fibers. The properties of the material can be described mathematically using complementarity relations involving the actual strain $\varepsilon_f(t)$, the Green strain $\varepsilon(t)$ and the viscoelastic stress $\tau(t)$:

$$\begin{aligned} \varepsilon_f(t) &\geq \varepsilon(t) - \bar{\varepsilon}_0, \\ \tau(t) &\geq 0, \\ \tau(t)\cdot(\varepsilon_f(t) - \varepsilon(t) + \bar{\varepsilon}_0) &= 0. \end{aligned} \tag{8}$$

Discretization of the problem results in following expressions:

$$\begin{aligned} \tilde{\tau}^{(n+1)} &= \frac{1}{c}[(1-\gamma)\sigma^{(n+1)} + \gamma(\exp(-\beta\Delta t)h^{(n)} \\ &\quad - \exp(-\beta\Delta t/2)\tau^{(n)})], \\ \tau^{(n+1)} &= \max\{0, \tilde{\tau}^{(n+1)}\}, \\ h^{(n+1)} &= \exp(-\beta\Delta t)h^{(n)} \\ &\quad - \exp(-\beta\Delta t/2)(\tau^{(n+1)} - \tau^{(n)}). \end{aligned} \tag{9}$$

Here $c = 1-\gamma\exp(-\beta\Delta t/2)$ and $\beta = 1/t_\sigma$. Thus, given the history parameter $h^{(n)}$, we first compute the trial tension $\hat{\tau}^{(n+1)}$. The complementarity relations (8) now yield the projection step $\tau^{(n+1)} = \max\{0, \tilde{\tau}^{(n+1)}\}$. Finally, we update the history parameter. For initialization of the recurrence we assume

$$\tau^{(0)} = (1-\gamma)\sigma^{(0)}, \quad h^{(0)} = 0. \tag{10}$$

Following form of the non-linear response was selected:

$$\sigma^{(n+1)} = D\exp[\kappa\varepsilon^{(n+1)} - \bar{\varepsilon}_0] - \sigma_0. \tag{11}$$

Here, vector $\varepsilon^{(n+1)}$ represents the known experimental values of the deformation of the material under consideration. Thus, we have six material parameters to determine: $\gamma, \sigma_0, \bar{\varepsilon}_0, D, \kappa$ and β.

Further, hyperelastic Mooney-Rivlin and Hart-Smith noncompressible models were applied. These models are characterized by the strain energy density functions w^m and w^h, respectively,

$$w^m = c_1(I_1-3) + c_2(I_2-3), \tag{12}$$

$$w^h = c_3\int \exp[c_4(I_1-3)^2]dI_1 + c_5\ln(I_2/3), \tag{13}$$

where $c_i, i = 1,\ldots,5$ are material moduli of the models and I_1, I_2, I_3 are the strain invariants of the right Cauchy-Green deformation tensor. The 2nd Piola-Kirchhoff stress tensor follows from $S_{ij} = \partial w/\partial\varepsilon_{ij}$, where w stands for the appropriate energy function and ε for strain.

Data identification was performed in MATLAB® using the built-in functions of the optimization toolbox; `lsqcurvefit` and `lsqnonlin` based on the least-squares method using Levenberg-Marquardt and/or large scale algorithm. For details, see [2].

Results & Discussion

A huge set of material parameters E_p, E_S^k and η^k that depend on the strain was identified for each specimen of estan and/or silicon. The generalized Maxwell models are regarded as linear and quasi-static in respect to each step of stretch. However, the stress and the moduli have, in general, a non-linear behaviour depending on the relative strain. For a better visualization of the resulting moduli, the values were fitted by polynomial, see Figure 7.

Estan moduli show approximately linear dependence on the relative strain up to 50% deformation. Parallel elastic modulus is a decreasing function of the strain while the serial moduli correspond to increasing function of the strain. The magnitude of the elastic moduli of estan is of the order of 10^6 Pa. Viscous moduli (damping) show linear character as well with the magnitude of 10^8 Pa·s.

Situation is more complicated in the case of silicon material. The linearity is no longer apparent in the case of silicon samples. The parallel modulus decrease up to 50% of strain, than remains almost constant up to 150% of strain and after this value it starts to increase. However, in contrast to estan samples, silicon specimens were

ISSN: 1727-1983

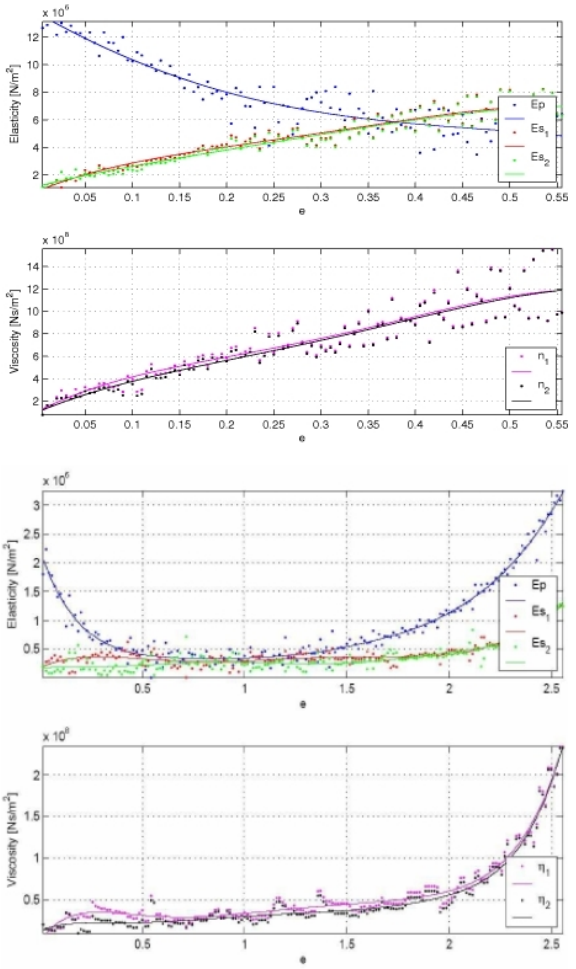

Figure 7: Estan (top) and silicon (bottom) moduli identified by fitting the experimental data with generalized 5-parameters Maxwell model.

stretched up to 250% of the initial length. Changing the scale of graph on the Figure 7 would show correspondance between estan and silicon material within the interval 0–50% of strain. The serial moduli are again increasing functions of the relative strain. The absolute values are smaller than those of estan, however, the magnitude is same, 10^6 Pa. The viscous moduli increase as well, the slope of the curve increase significantly beyond 200% of stretch. Again, the absolute values are smaller than in the case of estan but the magnitude remains same, 10^8Pa·s.

Non-linear model with slack length element was applied only to small part of the output data, i.e. to two stretch cycles. The identification uses large scale algorithm based on gradient methods; changing values of six material parameters demands huge computational capacity and large time intervals. This model is therefore not appropriate for large experimental data, however, the precision of the fitting is more than satisfactory and model allows to fit more than one step of stretch in contrast to previous linear Maxwell models. The stress-relaxation phenomena is fitted in more realistic way. Example of fitting of silicon experimental data is presented on the Figure 8. Table 1 shows material moduli of the non-linear

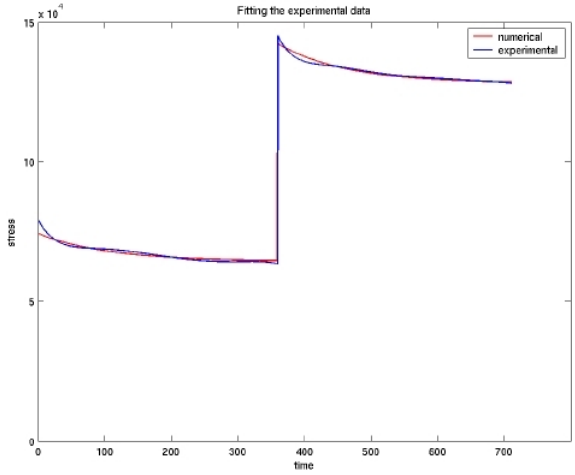

Figure 8: Fitting the experimental silicon data with non-linear viscoelastic model.

model with the slack length parameter determined for two steps of strech of a silicon sample.

Table 1: Non-linear material moduli of silicon.

D=$9.98 \cdot 10^5$ [Pa]	κ=69.31 [−]
σ_0=$1.01 \cdot 10^5$ [Pa]	ε_0=2.09 [−]
γ=0.18 [−]	β=0.79 [s^{-1}]

Finally, hyperelastic moduli were assessed. The example of the results of the fitting process are shown on the Figure 9. Stress-strain dependence was fitted by Mooney-Rivlin and Hart-Smith models that are defined by strain energy density functions (12) and (13), respectively.

Mooney-Rivlin model gives satisfactory results up to 180% of the initial length. After this value, the discrepancy between experimental data and numerical values from the fitting process is apparent. Behaviour of the material is more accurately characterized by Hart-Smith model. Experimental and numerical data correspond up to 280% of the initial length of the specimen. As an example of the material moduli determined, following may be mentioned: $c_1 = 111$ kPa, $c_2 = 226$ kPa, $c_3 = 246$ kPa, $c_4 = 14831$ [−] and $c_5 = 0.0298$ Pa.

Aorta strips cut in circumferential direction off the porcine abdominal aorta were tested in traction and the stress-strain dependence was registred up to possible rupture of the sample. Figure 10 shows measurement of three different samples in comparison to results available in literature [5]. Experimental curves show good consistency up to 140% of the initial length. However, significant discrepancy with the results presented in [5] is apparent but not surprising. The results from the experiments on soft tissue differs very often between laboratories in dependence on the method employed, conditions of the experiment etc.

ISSN: 1727-1983

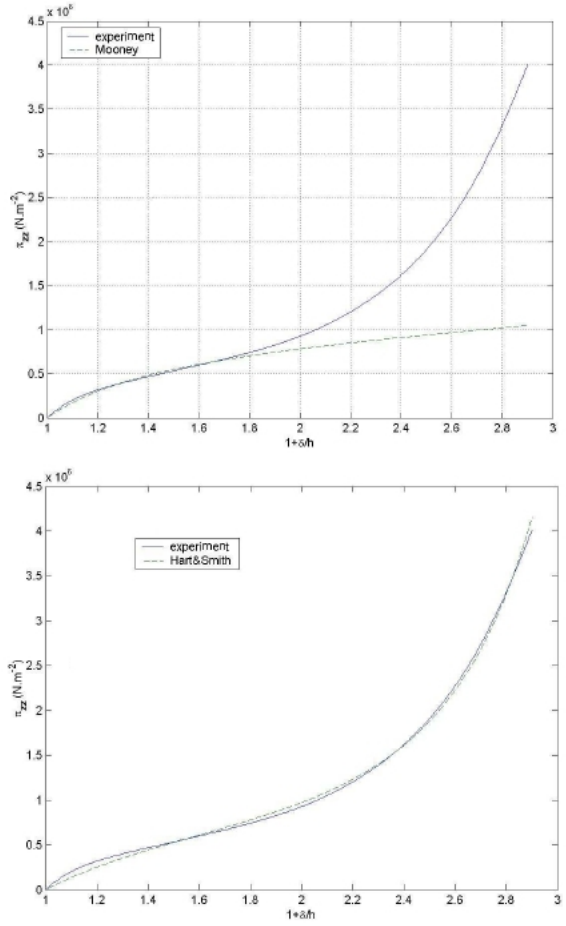

Figure 9: Fitting the experimental data with Mooney-Rivlin (top) and Hart-Smith (bottom) model.

Conclusion

Simple traction experiments were performed on estan and silicon materials in order to investigate the stress-relaxation phenomena. These materials are used to create the physical models of blood vessels for the experiments investigating blood flow. Three types of models were used to fit the experimental data. Firstly, generalized Maxwell viscoelastic model was used to fit the evolution of stress in time. The model fits the experimental data in each step of stretch independently; from this point of view, it is linear and quasi-static model. However, resulting moduli are approximately linearly dependent on the relative strain with the magnitude of elastic and viscous moduli of the orders of 10^6 Pa and 10^8 Pa·s, respectively. Secondly, non-linear viscoelastic model with the slack length element was applied. This model permits to fit precisely a number of stretching steps but demands huge computational capacity. Lastly, simple hyperelastic models were employed to fit the stress-strain relation. Mooney-Rivlin model gives good results up to 180% of the initial length. Hart-Smith model characterize very good behaviour of the material under consideration up to 280% of the initial length.

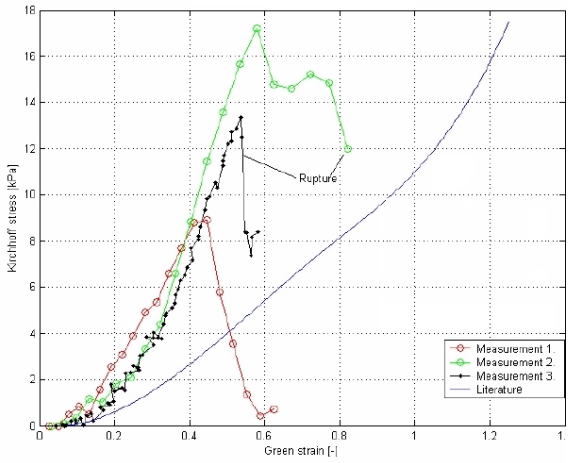

Figure 10: Stress-strain relation of porcine abdominal aorta.

Porcine abdominal aorta samples were examined as well. However, this part of the work is considered as a preliminary study. Stress-strain relation was measured and compared to data available in the literature. Measured data are in good agreement. Significant discrepancy is apparent when the data are compared with results presented in [5]. However, in the case of soft tissue, the results are not consistent very often between laboratories.

The authors would like to design a method for manufacturing suitable physical models of blood vessels for the PIV and UVP experiments that would respect various properties of real tissue based on the experiment presented in this work. This is a subject of future work.

Acknowledgement

This paper is sponsored by the pro ject of the Ministry of Education of the Czech Republic MSM 4977751303

References

[1] R. Cimrman. *Mathematical Modelling of Biological Tissues*. PhD thesis, University of West Bohemia, 2002.
[2] The MathWorks, Inc. *Matlab User Manual*.
[3] M. Orosz, G. Molnárka, M. Tóth, G.L. Nádasy, and E. Monos. Viscoelastic Behavior of Vascular Wall Simulated by Generalized Maxwell Models – A Comparative Study. *Med Sci Monit*, 5(3):549–555, 1999.
[4] E. Rohan. Mathematical Modelling of Soft Tissues, 2002. Habilitation Thesis.
[5] D.P. Sokolisa, H. Boudoulasb, and P.E. Karayannacosa. Assessment of the Aortic StressStrain Relation in Uniaxial Tension. *Accepted 16 April*, 2002.

ISSN: 1727-1983